The Brittle-to-Ductile Transition in Microlayer Composites

E. SHIN,* A. HILTNER,** and E. BAER

Department of Macromolecular Science and Center for Applied Polymer Research,
Case Western Reserve University, Cleveland, Ohio 44106

SYNOPSIS

The brittle-to-ductile transition in continuous microlayer composites of polycarbonate (PC) and styrene–acrylonitrile copolymer (SAN) was investigated under the triaxial tensile stress state achieved at a semicircular notch. The availability of microlayer compositions with variations in the proportion of the components and also variations in the total number of alternating layers made it possible to examine the transition from SAN-like, relatively brittle behavior, to PC-like properties where the ductile component dominated yield and failure. Examination of the damage zone that formed at the notch root revealed that cavitational mechanisms dominated in the brittle composites that were those with the highest proportion of SAN and fewest number of layers. Shear-yielding modes characteristic of PC dominated the damage zone of the ductile composites. Cavitational mechanisms were almost totally absent in these compositions that included those with the highest proportion of PC and the largest number of layers. A broad range of transitional behavior was observed with intermediate compositions where elements of both cavitational mechanisms and shear modes were superimposed. These compositions provided an opportunity to examine the interaction of cavitational and shear processes at the macro- and microscales. © 1993 John Wiley & Sons, Inc.

INTRODUCTION

Shin, Hiltner, and Baer[1] described the irreversible deformation behavior of coextruded microlayer composites consisting of 49 alternating layers of PC and SAN. Deformation was examined in the triaxial tensile stress state achieved at a semicircular notch during slow tensile loading. Variations in the proportions of PC and SAN were manifested as changes in the relative thicknesses of PC and SAN layers. Compositions that were highest in SAN were only slightly more ductile than SAN, and the damage zone that formed at the notch tip during loading resembled that of SAN which consisted of internal notch crazes in the SAN layers that grew out from the notch surface in conformity with a mean-stress condition. Shear processes in both PC and SAN lay-

ers became more evident as the proportion of PC increased, but failure and fracture were dominated by the relatively brittle SAN component in the 49-layer composites.

It is possible to decrease the layer thickness of microlayer composites by increasing the total number of alternating layers. It has been observed that when the number of layers is increased from 49 to 776 while maintaining the sheet thickness constant, mechanical properties such as ductility and toughness are improved for any given PC/SAN ratio.[2,3] Good adhesion between PC and SAN creates the possibility for extensive interaction, and it appears that brittle fracture of the SAN layers is suppressed when the layer thickness is decreased from tens of microns to the micron-size scale. The availability of microlayer composites with different numbers of layers and different compositions made it possible to examine the transition from SAN-like, relatively brittle behavior, to PC-like properties where the ductile component dominates the yield and failure characteristics of the entire system. Observations of the damage zone that formed in uniform tension at

a semicircular notch were compared at the macro- and microscales with previous descriptions of SAN[4] and PC.[5]

EXPERIMENTAL

The microlayer composites (The Dow Chemical Company) were 1.2 mm-thick coextruded sheet.[1-3,6] The sheets consisted of 49, 194, 388, or 776 alternating layers of PC and SAN. The outermost layer was PC in all cases. Nominal compositions taken from the feed rates to the extruders were provided by Dow (Table I). The composition on a volume basis was determined directly from micrographs by measuring the thickness of individual layers in cross sections through the thickness. Since the thickness of individual SAN and PC layers sometimes varied somewhat from the edge to the center of the sheet, values of the composition and layer thickness reported in Table I are averages. These values were used when required in calculations.

Tensile tests of notched rectangular specimens 100 mm × 20 mm with a single 1 mm-radius, semicircular notch were carried out on an Instron Testing Machine. The damage zone at the notch was photographed during deformation with a traveling optical microscope in the transmission mode. In some cases, specimens were loaded to specific positions on the stress-displacement curve and removed from the Instron for further characterization of the damage zone. Details of the experimental procedures were described previously.[1,4]

RESULTS

Stress-Displacement Curves

The stress-displacement curves of all the multilayered compositions were less brittle than SAN but also less ductile than PC. The slopes of the initial linear region, which were related to the moduli, were distributed between those of SAN and PC. Failure and fracture behavior was also intermediate. As a general trend, the stress and extension at fracture increased with the proportion of PC in the composite; but the layer thickness also had an effect and, for a given composition, the fracture parameters increased as the number of layers increased.

It was convenient to categorize the composites by their extension at fracture. The Type I brittle and Type II "semi-brittle" compositions all fractured at higher stresses and extensions than SAN, but they fractured before reaching a maximum in the stress-displacement curve. The Type I brittle composites fractured at extensions below 1.8 mm. The maximum extension of the Type II semi-brittle compositions was between 1.8 and 2.5 mm. The Type I and Type II composites included those with the highest proportion of SAN and the fewest number of layers.

Table I Microlayer Compositions and Mechanical Data

	Composition PC/SAN v % (Layer Thickness μm)		Young's Modulus, E^a (GPa)	Poisson's Ratio, ν^a
Layer	As Given	As Measured		
49	27/73	25/75 (11/34)	3.11	0.363
	40/60	53/47 (23/22)	2.86	0.377
	54/46	65/35 (27/15)	2.75	0.383
	65/35	74/26 (33/13)	2.67	0.387
194	26/74	30/70 (3.6/8.2)	3.07	0.365
	40/60	45/55 (4.9/5.4)	2.93	0.372
	77/23	76/24 (8.9/2.9)	2.67	0.388
388	47/53	53/47 (3.6/3.3)	2.86	0.377
776	35/65	40/60 (1.3/2.0)	2.97	0.370
	50/50	55/45 (1.5/1.2)	2.84	0.378
	65/35	67/33 (1.9/1.0)	2.73	0.384
	SAN[b]		3.34	0.35
	PC[b]		2.43	0.40

[a] Calculated by the Rule of Mixtures.[1]
[b] Experimental data.[6]

Three of the higher PC composites were differentiated from the others by a maximum in the stress-displacement curve, and in this regard the stress-displacement curves resembled that of PC although the extensions were not as high. These Type III "ductile" composites were also ones with the larger number of layers. Although the composites were categorized here on the basis of bulk mechanical behavior, each Type also correlated with certain characteristics of the damage zone that developed in front of the notch during deformation.

Damage Zone of Type I Brittle Composites

Three composites were classified as Type I: the 194-layer composite with the highest SAN content and the two 49-layer composites with the highest SAN contents. The stress-displacement curves are compared in Figure 1. The stress and displacement at fracture were higher for the composites than for SAN, but the shape of the stress-displacement curves was very similar. The onset of nonlinearity coincided with the initiation of a craze zone at the notch surface, and the nonlinear region was characterized by lengthening of the crazes away from the notch. Although the adhesion between PC and SAN layers was good, at higher stresses the craze lines thickened and darkened somewhat suggesting that some microdelamination at the SAN–PC interface occurred. Just prior to fracture, a macrodelamination crack appeared at the notch tip and subsequent fracture occurred rapidly leaving a relatively smooth brittle-fracture surface.

Characteristic Type I behavior is illustrated with data for the PC/SAN 30/70 (194 layers) composite. Micrographs of the damage zone at two positions on the stress-displacement curve are shown in Figure 2. The damage zone that formed at the notch in the Type I brittle compositions consisted of continuous internal notch crazes in the SAN layers emanating from the notch surface.[1] The crazes were similar to those observed in SAN,[4] but were much denser in the multilayer composites and, furthermore, while the crazes followed straight lines in SAN, they were slightly curved in the composites.

A cross section of the damage zone in the PC/SAN 30/70 (194 layers) composition loaded to 35 MPa is shown in Figure 3(a). The section, which was made about 20 μm from the notch tip, shows crazes more or less uniformly distributed in the SAN layers through the thickness of the composite. Although most of the crazes were isolated with no registry from one SAN layer to the next, occasionally crazes appeared in small arrays with crazes aligned perpendicular to the stress in two or three neighboring SAN layers. Arrays of internal-notch crazes were not observed in 49-layer composites.[1]

Another cross section, this one of a specimen that had been loaded to 44.1 MPa and microtomed 200 μm from the notch tip, again showed the crazing in SAN layers and additionally, microshear bands in the PC layers that had initiated from the craze tips [Fig. 3(b)]. This composition fractured when the stress was 45.5 MPa, only slightly higher than at position 2. A cross section through the fracture surface close to the notch tip [Fig. 3(c)] showed very
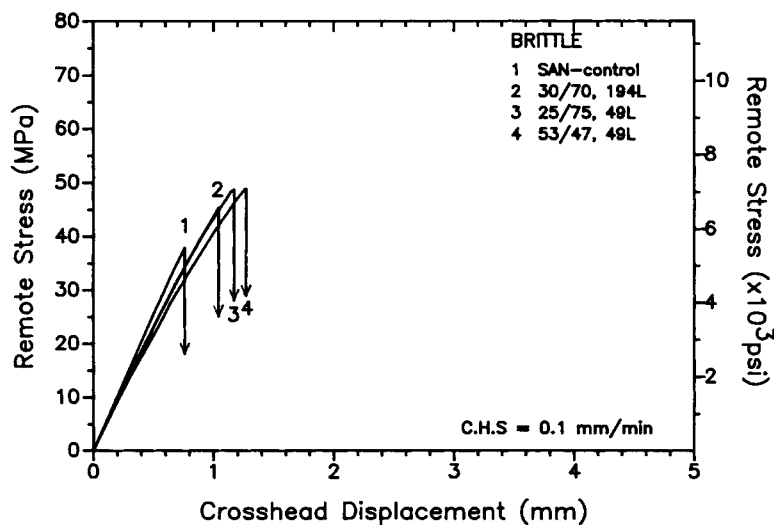
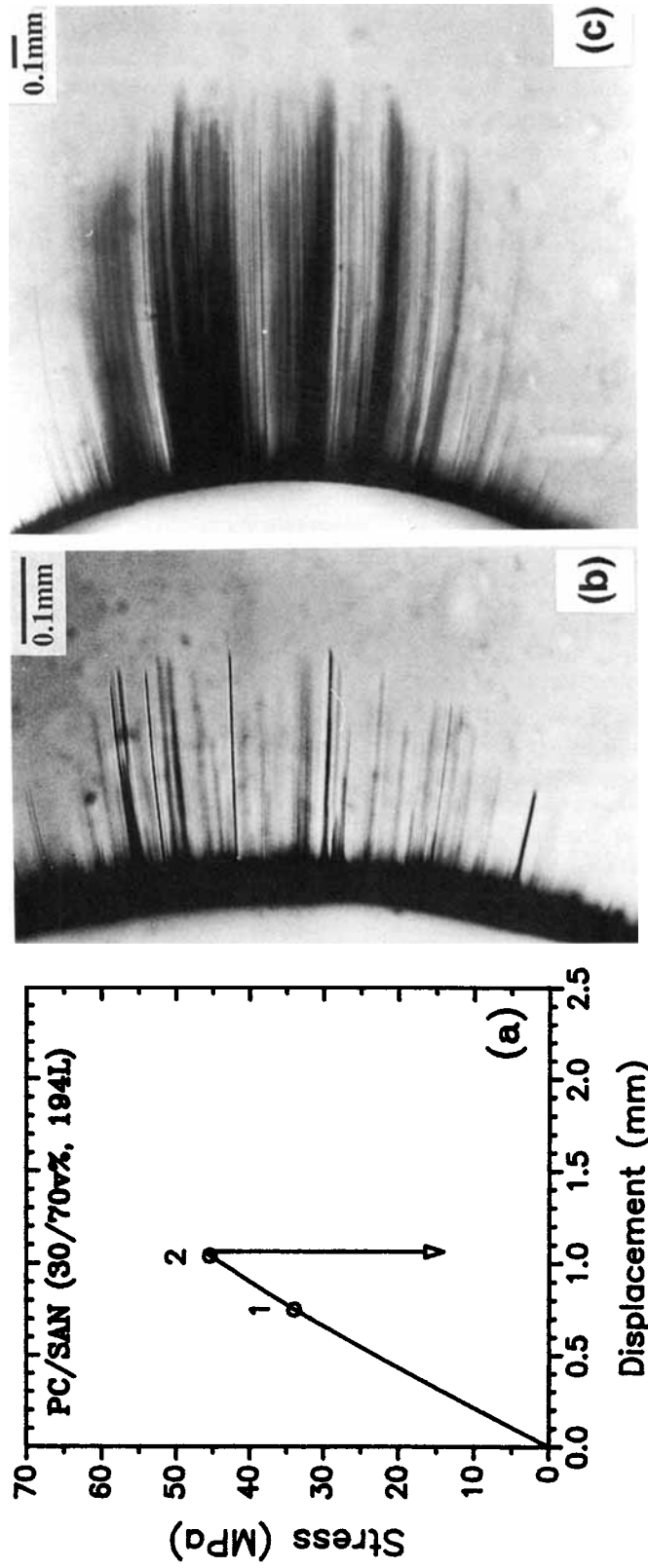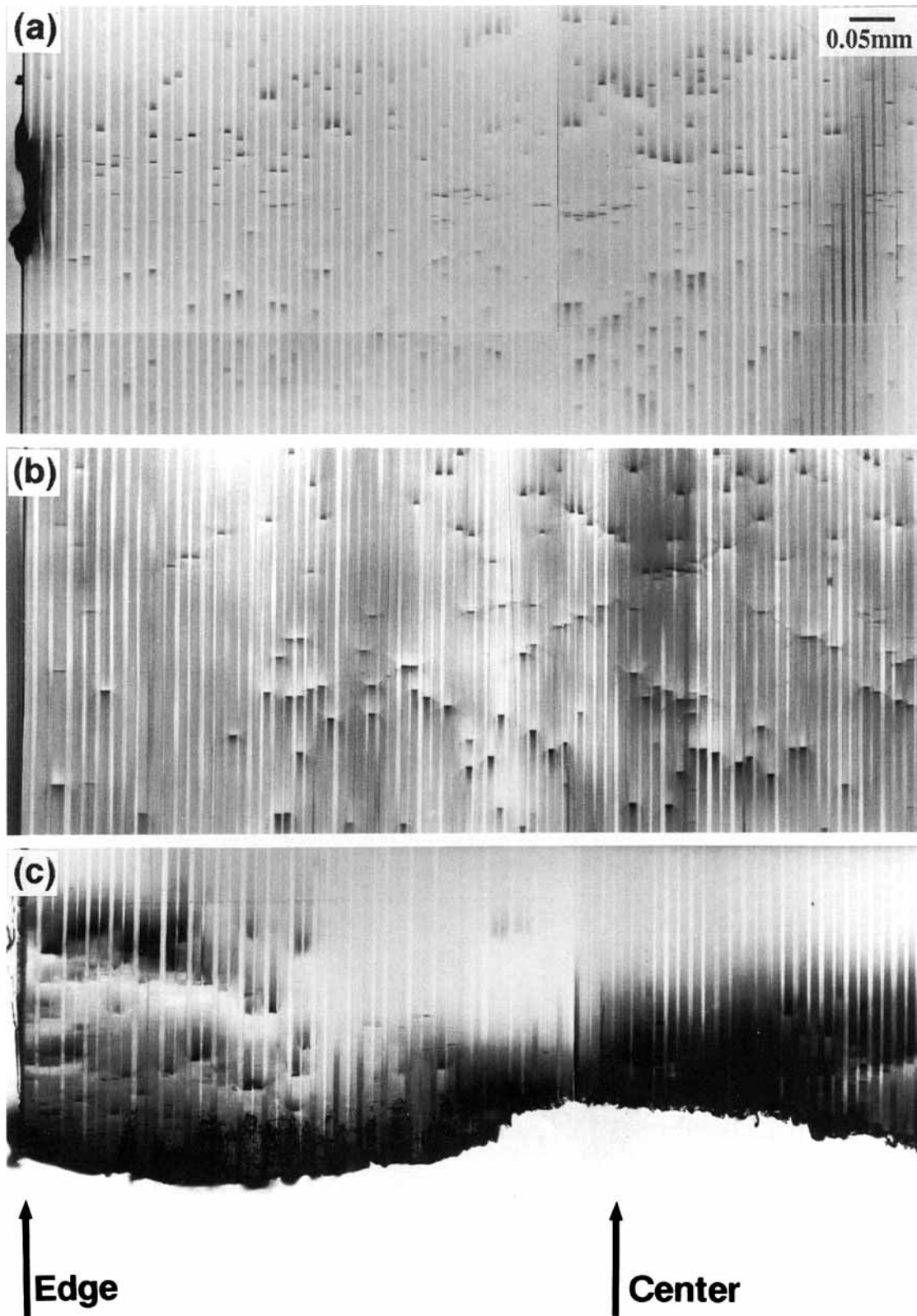**Figure 1** Stress-displacement curves of the three brittle microlayer composites compared with SAN.

Figure 2   Tensile deformation of PC/SAN 30/70 (194 layers) with a semicircular notch. (a) The stress-displacement curve; (b) optical micrograph of the damage zone at the notch tip at position 1, 33.9 MPa; and (c) optical micrograph at position 2, 45.4 MPa.

0.05mm

Edge   Center

Figure 3 Microtomed cross sections of the damage zone of PC/SAN 30/70 (194 layers). (a) Loaded to 35 MPa with a displacement of 0.79 mm and microtomed 20 μm from the notch root; (b) loaded to 44.1 MPa with a displacement of 1.0 mm and microtomed 200 μm from the notch root; and (c) a fractured specimen microtomed 10 μm from the notch root.
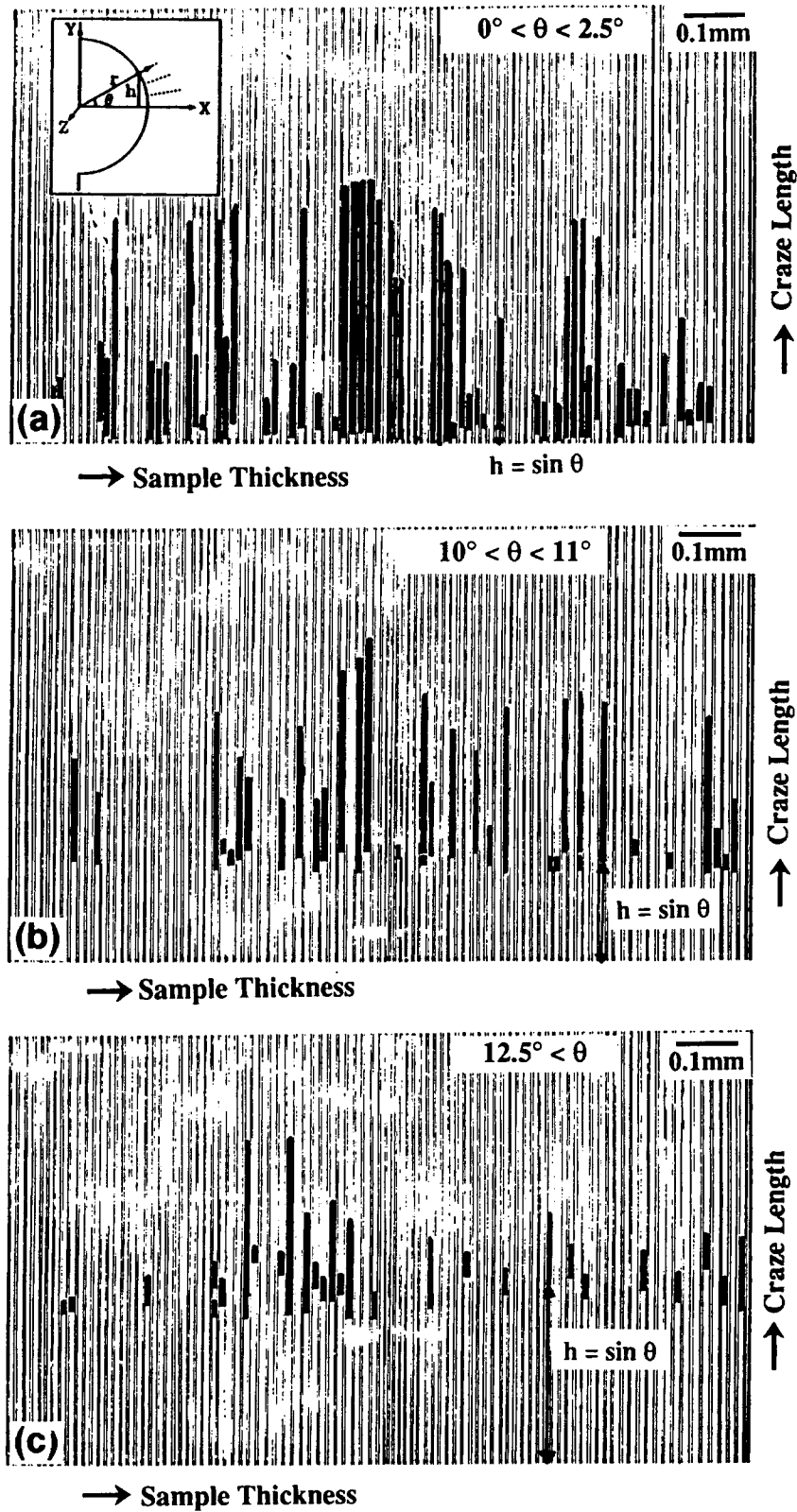
Figure 4   Profiles of internal-notch crazes in PC/SAN 30/70 (194 layers) loaded to 35 MPa. (a) Crazes in the center of the damage zone close to the x-axis; (b) crazes located between the x-axis and the edge of the damage zone; and (c) crazes near the edge of the damage zone.

little additional plastic deformation in the vicinity of the crack path and both PC and SAN layers fractured in a brittle manner.

Profiles of the internal notch crazes that comprised the damage zone of the PC/SAN 30/70 (194 layers) composite at 35 MPa were constructed by locating each craze in successive cross sections.[1-4] The point of craze initiation on the notch surface was identified by the perpendicular distance from the x-axis given by h (mm) = sin θ [insert, Fig. 4(a)]. Crazes with growth planes close to the x-axis ($\theta \sim 0$) [Fig. 4(a)], included the longest crazes, although there were also a number of shorter crazes. Crazes of intermediate length were located midway between the x-axis and the boundary of the damage zone ($\theta \sim 10°$) [Fig. 4(b)], and the shortest crazes were near the boundary of the zone ($\theta > 12°$) [Fig. 4(c)].

While craze length was strongly dependent on the angle θ, especially when the zone was small, examination of the sequential cross sections revealed no general trends in the thickness direction; rather, craze length and craze density were much the same through the thickness except in the few SAN layers closest to the edges where there were almost no crazes. This suggested that except close to the edges, the SAN layers were in a triaxial stress state that did not vary through the thickness. It is unusual to associate the plane-strain state with thin layers. However in this situation, constraint in the thickness direction was provided by good adhesion between the alternating SAN and PC layers.
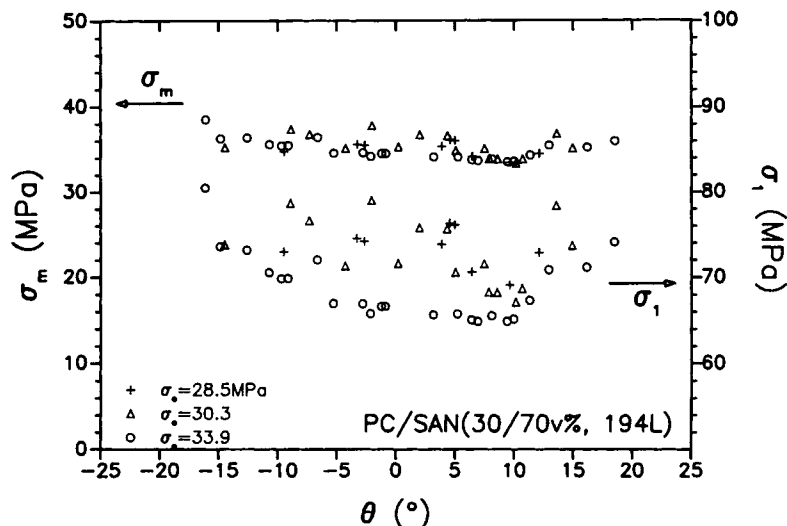
The positions of the craze tips at various remote stresses are plotted in Figure 5. As previously observed in both SAN and the 49-layer composites, the damage zone defined by the tips of the internal crazes was initially crescent shaped, but as the remote stress increased, the damage zone gradually took on a more elongated shape. Assuming the composite could be treated as a linear elastic solid when the zone was small, the classical elastic stress distribution at a single semicircular notch from Maunsell's solution was used to analyze the stress state at the craze tips.[7] The values of both the major principal stress (σ_1) and the mean stress (σ_m) at the tip of each internal-notch craze are plotted as a function of the angle θ in Figure 6. As was the case previously, the stress state at the craze tip conformed closely to a constant mean-stress condition when the zone was small, while the major principal stress exhibited a decreasing trend from the edge of the zone to the center. The critical mean stress $\sigma_{m,c}$ is given in Table II together with values for the 49-layer composites.

It is possible for crazes in SAN to follow either σ_2-trajectories or σ_2-vectors.[4] Craze trajectories in the microlayer composites were not straight but curved away from the notch as they lengthened. The craze trajectories were compared with the two limiting cases by plotting the craze slope, defined as the slope of the tangent to the craze line at any point on the craze, normalized to tan θ. Only crazes that initiated at positions described by larger θ angles were analyzed since both σ_2-vectors and minor principal stress trajectories were nearly parallel to the x-axis when θ was with ±10°. Internal-notch crazes in SAN followed σ_2-vectors where local stress redis-
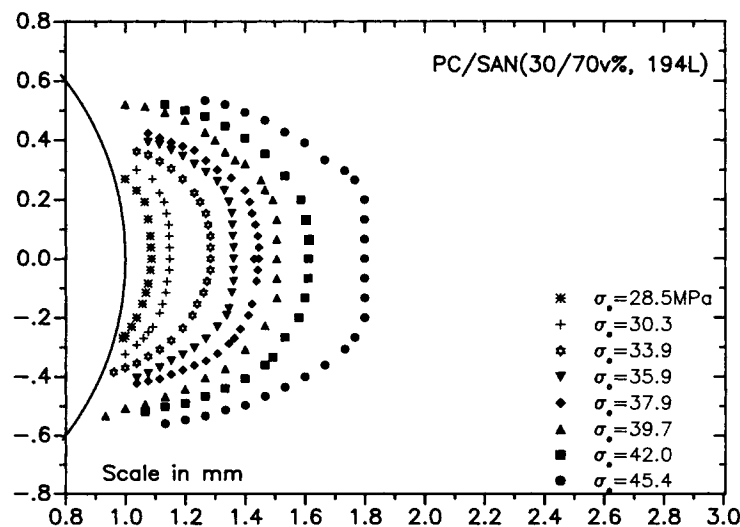
Figure 5   Positions of the internal-notch craze tips for PC/SAN 30/70 (194 layers) at several remote stresses.

Figure 6 Mean stress (σ_m) and major principal stress (σ_1) at the positions of the craze tips for PC/SAN 30/70 (194 layers) at lower remote stresses as a function of the angle θ.

tribution caused by the presence of the craze was thought to control the craze trajectory.[4] Craze trajectories in PC/SAN 30/70 (194 layers) were intermediate between the σ_2-vectors and the σ_2-trajectories (Fig. 7). When this characteristic of the craze trajectories was observed in 49-layer composites, it was suggested that constraint by the PC layers partially offset local stress redistribution in the SAN layers.[1]

Damage Zone in Type II Semi-Brittle Composites

The Type II semi-brittle compositions also fractured before reaching a maximum in the stress-displacement curve (Fig. 8), but these composites exhibited a longer nonlinear region in the stress-displacement

curve and higher fracture stress and strain than the Type I brittle composites. The composites in this category exhibited behavior that was transitional from SAN-like to PC-like. The range of Type II behavior is illustrated with two composites of similar composition but different number of layers, PC/ SAN 45/55 (194 layers) and PC/SAN 53/47 (388 layers).

A family of internal-notch crazes was again the first damage observed in these compositions (Fig. 9). The initial crescent shape of the damage zone defined by the craze tips in the PC/SAN 45/55 (194 layers) composite was the same as in the brittle compositions. As the zone grew away from the notch at higher stresses, the crazes near the edge of the zone were nearly the same length as the crazes that

**Table II Critical Conditions for Internal-Notch Crazes in PC/SAN Composites**

Composition (PC/SAN v %, No. of Layers)	$\sigma_{m,c}$ (MPa)		V_c (%)	
	Average	Local (SAN)[a]	Average	Local (SAN)[a]
SAN[b]	35.1	35.1	0.95	0.95
25/75, 49[c]	33.0	35.4	0.87	0.95
53/47, 49[c]	31.0	36.2	0.80	0.97
65/35, 49[c]	29.2	35.5	0.75	0.96
30/70, 194	34.6	37.3	0.92	1.00
45/55, 194	34.9	39.2	0.92	1.05

[a] Critical values calculated for SAN layer using the Rule of Mixtures,[1]
[b] Shin, Hiltner, and Baer.[4]
[c] Shin, Hiltner, and Baer.[1]
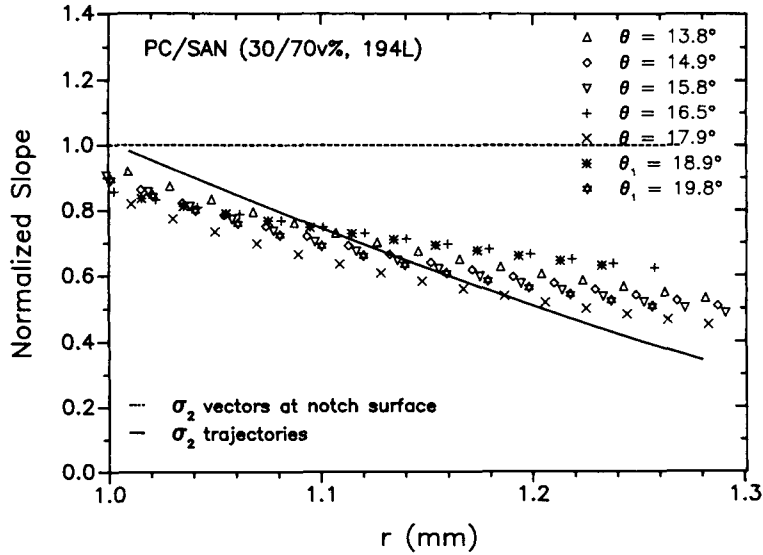
Figure 7 The slope of internal notch crazes in PC/SAN 30/70 (194 layers) normalized to the slope of the σ_2-vector at the position of craze initiation on the notch surface.

grew close to the x-axis. This imparted a rather blunt shape to the craze zone compared to the more ovoid shape of the zone in the brittle compositions. The zone also grew to be longer than in the brittle compositions that reflected the higher extension at fracture. Curvature of the crazes near the edge of the zone was again evident. The crazes were long enough in this composition to clearly show that they curved over and grew almost parallel to the x-axis. The crazes followed trajectories that were very similar to those in the Type I brittle composites; the trajectories were again intermediate between the σ_2-vectors and the σ_2-trajectories.

While most of the crazes grew away from the notch as the stress increased, a few of the crazes ceased to grow. Closer examination revealed that these crazes terminated in a pair of microshear bands that grew into the SAN layer ahead of the craze. Sometimes, additional crazes initiated in the SAN layers but they initiated some distance ahead of the notch rather than at the notch surface. This phenomenon of near-notch crazing was more evident in the PC/SAN 53/47 (388 layers) composite (Fig. 10). The initial damage was again internal-notch crazing in the SAN layers, but the craze zone had a very ragged shape caused by the various lengths of
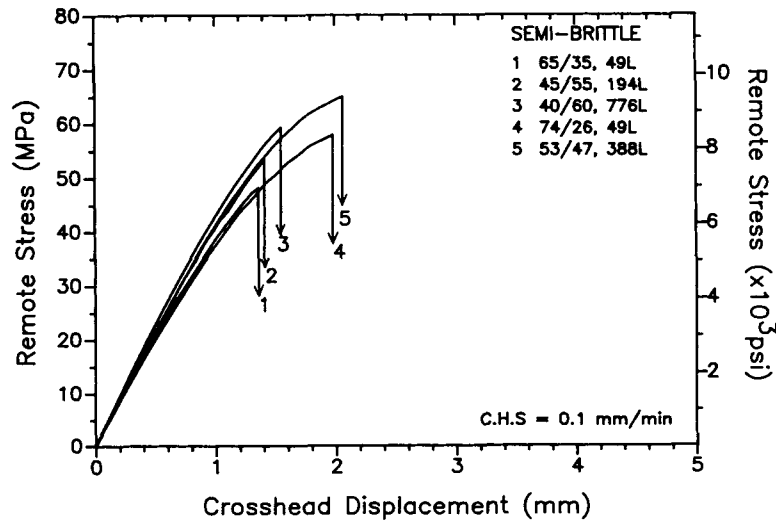
Figure 8 Stress-displacement curves of the five semi-brittle composites.
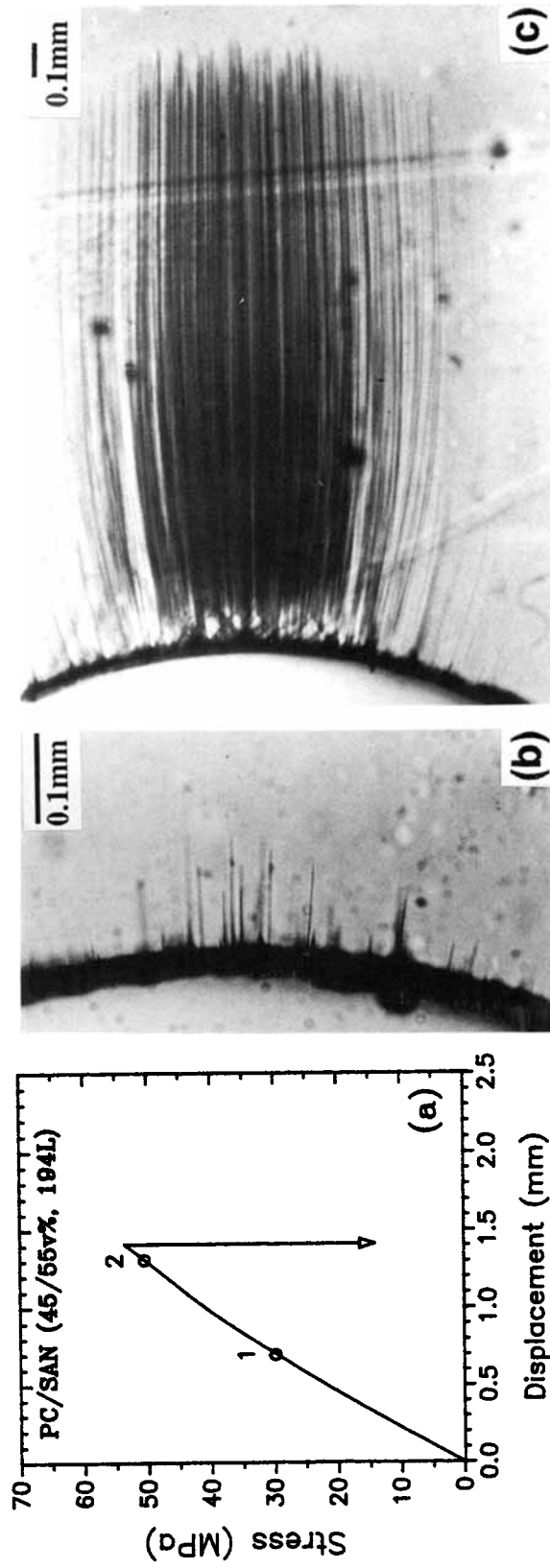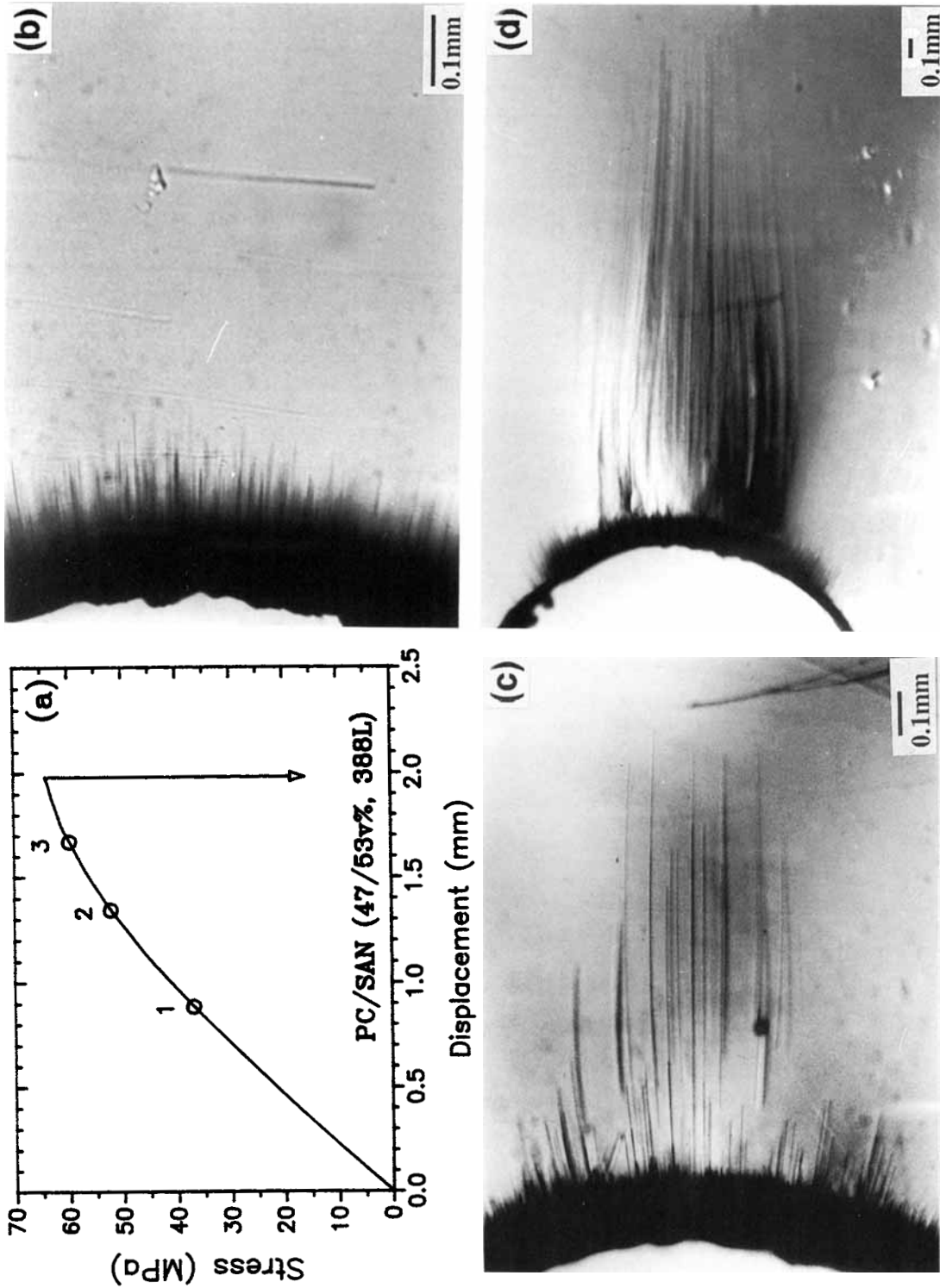
Figure 10 Tensile deformation of PC/SAN 53/47 (388 layers) with a semicircular notch. (a) The stress-displacement curve; (b) optical micrograph of the damage zone at the notch tip at position 1, 36.9 MPa; (c) optical micrograph at position 2, 52.1 MPa; and (d) optical micrograph at position 3, 59.7 MPa.

the crazes when they terminated in microshear bands in the SAN layer. None of the notch crazes grew more than a short distance from the notch surface. Instead near-notch crazes initiated ahead of the notch and grew away from the notch as the stress increased. The positions of the near-notch craze tips at several remote stresses are plotted in Figure 11 for PC/SAN 53/47 (388 layers). Intersection of the curve that described the craze boundary further from the notch with the position of the boundary near the notch suggested that near-notch crazes initiated in this composite at a remote stress of approximately 43 MPa.

All the Type II composites exhibited both types of crazing behavior in the SAN layers and only differed in the matter of degree. In the Type II composites with the lower fracture extensions, such as PC/SAN 45/55 (194 layers), growth of internal-notch crazes predominated and relatively few terminated in shear bands close to the notch surface, compared to the more ductile Type II composites such as PC/SAN 53/47 (388 layers) where many of the internal-notch crazes terminated after growing only a short distance away from the notch and the second family of internal crazes that initiated near the notch tip were more numerous.

Internal-notch crazing predominated in two of the Type II composites, and for these it was possible to determine the critical mean stress from the positions of the craze tips when the zone was small. Values of $\sigma_{m,c}$ are included in Table II along with values for the Type I brittle compositions.

Previously[1] when the rule of mixtures was used to obtain the local critical mean stress in the SAN layers of 49-layer composites, the local critical condition was observed to be independent of composition, and the average values of 35.5 MPa for $\sigma_{m,c}$ and 0.96 for the corresponding volume strain did not differ significantly from the critical conditions for internal notch crazing of SAN.[4] The same analysis of the 194-layer composites led to values of both average and local critical mean stress that were larger than the values for 49-layer composites although the compositions were similar. It was possible that craze initiation and/or growth required higher stresses when forced to occur under sufficiently confined conditions. However, the possibility could not be neglected that when the layers became thin enough, the simple rule of mixtures did not hold and the elastic stresses could not be assumed to be additive. Because of good adhesion, elastic-stress redistribution in the vicinity of the interface could not be neglected if it occurred over a distance comparable to the layer thickness. The stress in the SAN layers calculated by the simple rule of mixtures calculation would have been higher than the true stress. Regardless of the explanation, it remained that as the SAN layers became thinner, higher remote stresses were required for crazing.

A major difference between the Type I and Type II composites was the observation of a macroscopic shear-yielding mode in the Type II composites. At higher stresses, the two sets of intersecting slip lines that are characteristic of the core-yielding mode in
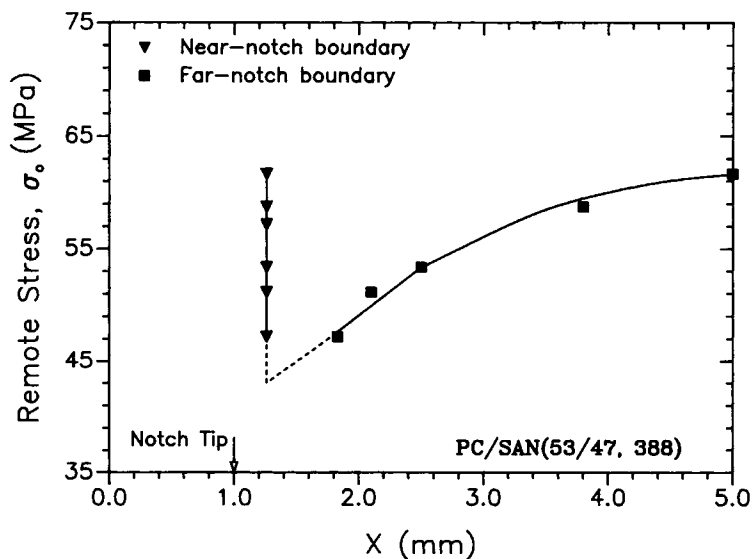
Figure 11 Positions of the near-notch craze tips in PC/SAN 53/47 (388 layers) at several remote stresses.
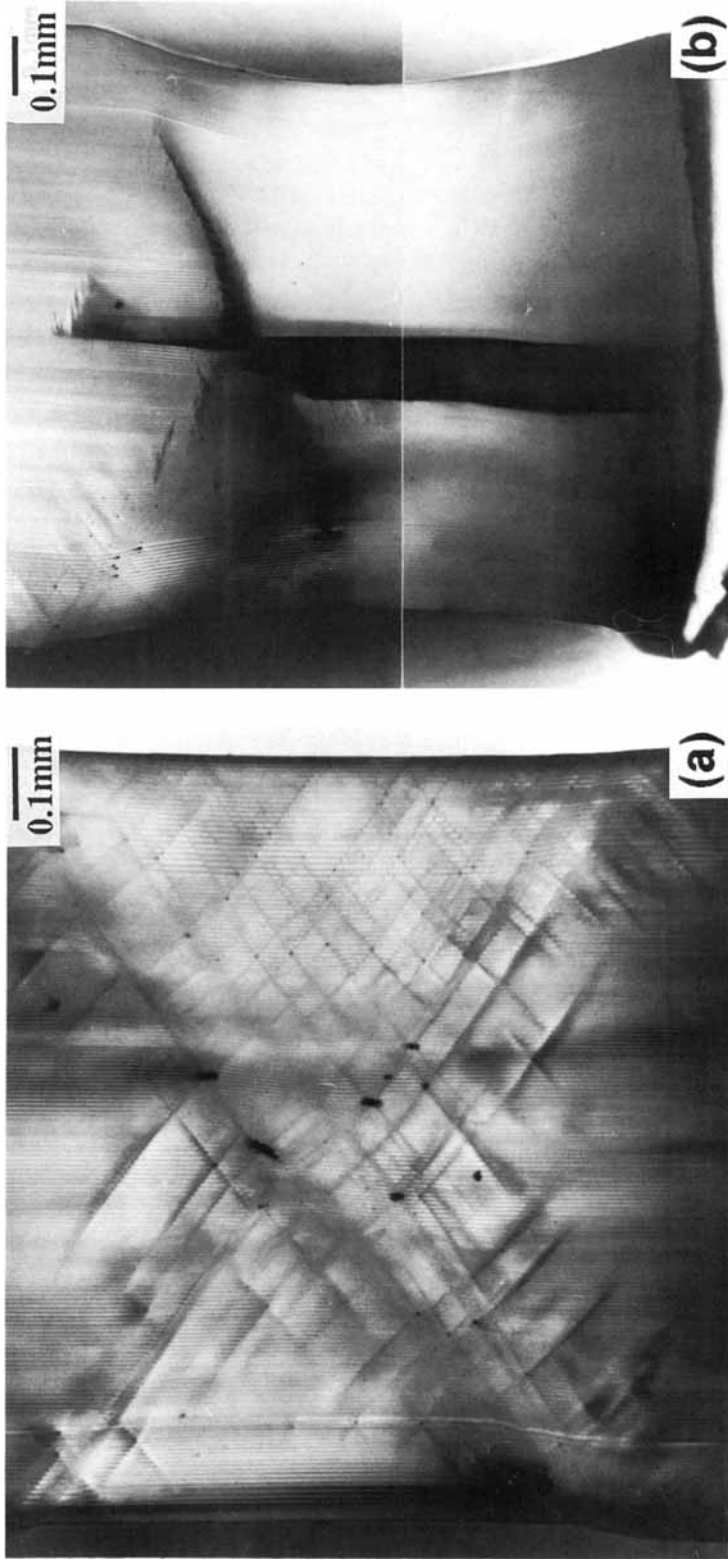
Figure 12 Microtomed cross sections of PC/SAN 53/47 (388 layers). (a) Loaded almost to fracture at 65.3 MPa with a displacement of 1.94 mm and microtomed 650 μm from the notch root; and (b) a fractured specimen microtomed 300 μm from the notch root.

PC[5] were visible at the notch root. Interaction of the PC core-yielding mode with SAN crazing was thought to cause the second family of internal near-notch crazes that appeared ahead of the notch near the position of the tip of the core-yielding zone. These crazes initiated in the SAN layers in response to the dilational stress concentration created by the presence of the plastic zone.

A second macroscopic shear-yielding mode was observed at higher stresses in the more ductile PC/SAN 53/47 (388 layers) composite that was not observed in PC/SAN 45/55 (194 layers). Intersecting shear, a through-thickness, shear-yielding mode that is also characteristic of thin polycarbonate sheet, produced thinning of the cross section. This shear mode was visible in optical micrographs as a pair of dark bands that grew out from the notch surface above and below the x-axis.

A cross section of a PC/SAN 53/47 (388 layers) specimen loaded almost to fracture at 65.3 MPa [Fig. 12(a)], shows a network of microshear bands that initiated from the near-notch crazes and grew through alternating PC and SAN layers. The microshear bands had begun to coalesce at an angle through the thickness into intersecting macroscopic flow lines. This intersecting shear mode led to the beginning of global necking of both PC and SAN layers, but the cross section of the fractured specimen in Figure 12(b) shows that the neck was not stable and fracture occurred in a region undergoing large local deformation at one end of the incipient neck. A center delamination crack is also seen in Figure 12(b). Formation of a delamination crack at

higher stresses near the tip of the core-yielding zone was characteristic of the Type II semi-brittle composites.

Damage Zone of Type III Ductile Composites

Three microlayer compositions resembled PC by exhibiting a maximum in the stress-displacement curve (Fig. 13), with necking and a slow tearing mode of fracture that resulted in a complex fracture surface. Internal notch crazes initiated at the notch surface but did not propagate very far from the notch in these composites. A second family of internal near-notch crazes was apparent in the ductile PC/SAN 76/24 (194 layers) composite (Fig. 14). The number decreased to only a few isolated near-notch crazes in the PC/SAN 65/35 (776 layers) composite and none were evident in the PC/SAN 77/23 (776 layers) composite. The third cavitational mechanism, delamination, was not observed in any of the ductile compositions.

The near-notch crazes initiated in the SAN layers in response to the dilational stress concentration created by the presence of a plastic zone at the notch root. Near-notch crazing was the primary crazing mode in five compositions, three Type II semi-brittle composites, and two Type III ductile composites. It was characteristic of these crazes that they propagated only away from the notch, not toward the notch. The position of the craze boundary near the notch was determined for each of the compositions that exhibited this type of crazing. Comparison of the values in Table III suggested an inverse rela-
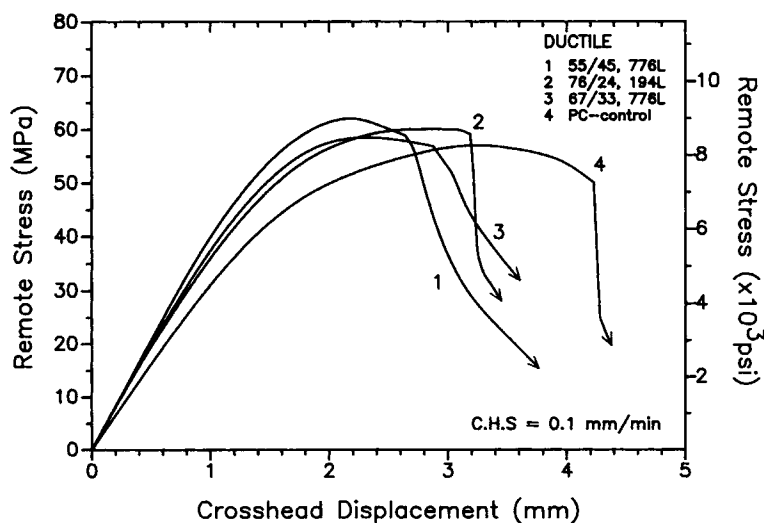
Figure 13 Stress-displacement curves of the three ductile composites compared with polycarbonate.
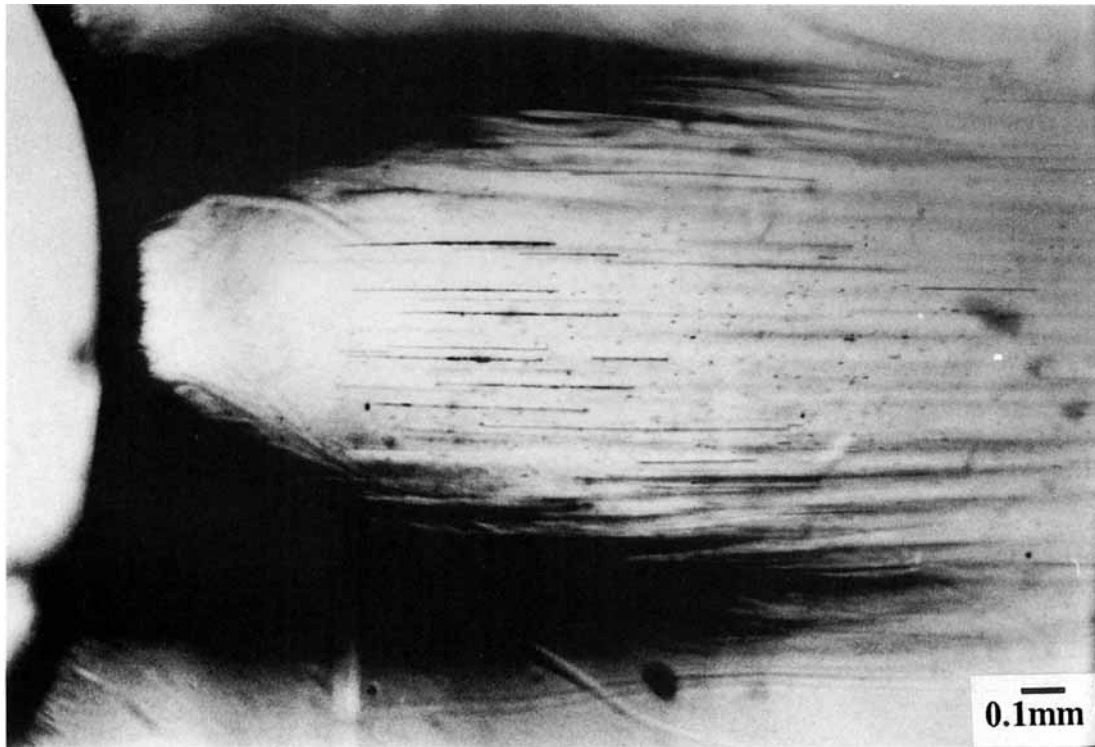
Figure 14   The damage zone of PC/SAN 76/24 (194 layers) loaded to 55.2 MPa and a displacement of 1.79 mm.

tionship between the thickness of the SAN layers and the distance of the crazes tips from the notch.

The local mean stress at the boundary of the near-notch craze tips was obtained from the plastic stress distribution in the core-yielding zone taking into account the pressure-dependent yield behavior of polymers.[8] As pointed out previously,[1] the analysis describes a homogeneous plastic zone and caution is required in interpreting the values of $\sigma_{m,c}$ in Table III. However, the increase in the average $\sigma_{m,c}$ from 37.3 MPa when the SAN layers were 13 μm thick, a value comparable to those obtained from the elastic analysis of the crescent-shaped craze zone in the

more brittle composites, to 50.8 MPa when the SAN layers were an order of magnitude thinner at 1.2 μm, suggested that crazing became increasingly difficult as the layer thickness decreased until the composite with the thinnest SAN layers, 1.1 μm in PC/SAN 67/33 (776 layers), did not exhibit any near-notch crazing. This trend may have occurred because the stress distribution increasingly departed from the simple rule of mixtures as the layers became thinner. If this were the case, stress redistribution would have caused the real stress in the SAN layers to be lower than the stress calculated by the simple rule of mixtures. Hence a higher remote stress would have been

Table III   Critical Conditions for Internal Near-Notch Crazes in PC/SAN Composites

Composites (PC/SAN v %, No. of Layers)	Pressure Coefficient, μ	SAN Layer (μm)	Near-Notch Boundary (mm From Notch Tip)	$\sigma_{m,c}$ (MPa)	
				Average	Local (SAN)
74/26, 49	0.1	13	0.1	37.3	46.7
53/47, 388	0.121	3.3	0.26	45.1	52.7
76/24, 194	0.096	2.9	0.28	45.8	57.3
40/60, 776	0.135	2.0	0.30	47.5	53.4
55/45, 776	0.119	1.2	0.38	50.8	59.7
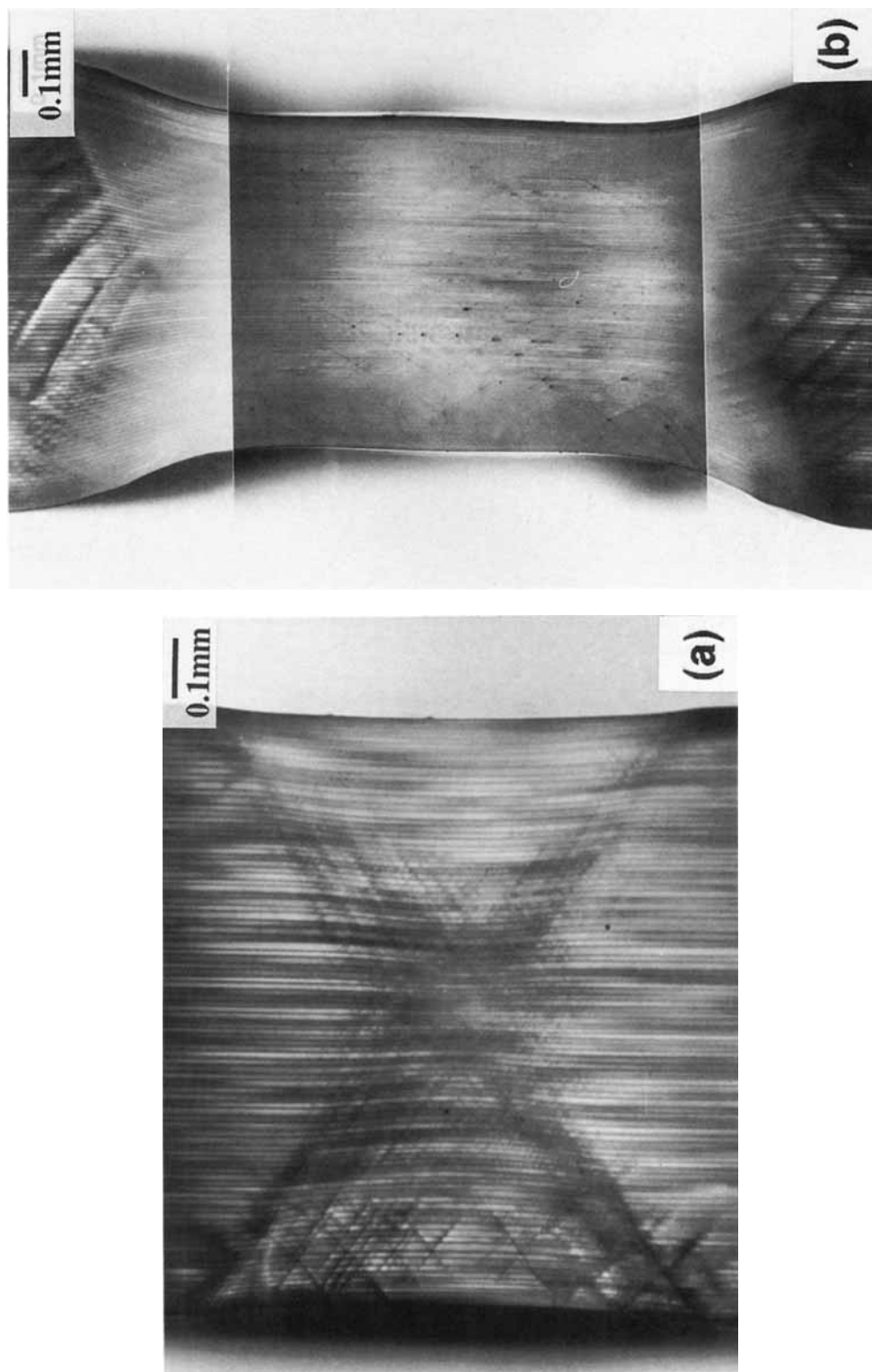
Figure 15   Microtomed cross sections through the damage zone of PC/SAN 76/24 (194 layers). (a) A specimen loaded to 57.4 MPa with a displacement of 1.92 mm and microtomed 500 μm from the notch root; and (b) loaded to 60.3 MPa with a displacement of 2.64 mm and microtomed 550 μm from the notch root.

required for the craze condition to be achieved in the SAN layers.

Shear-yielding modes dominated the damage zone of the ductile composites. The intersecting slip lines of core yielding could be seen at the notch root, but at higher stresses the dominant feature in micrographs of the damage zone was the pair of dark bands of the intersecting shear mode that grew out from the notch surface above and below the x-axis. A cross section of the damage zone formed at 57.4 MPa, only a slightly higher stress than that used to produce the damage zone in Figure 14, shows that microshear bands initiated at crazes in the SAN layers and grew away from the craze through alternating PC and SAN layers [Fig. 15(a)]. The microshear bands coalesced to create the continuous macroscopic through-thickness flow lines of intersecting shear that followed the same angle, 53° to the y-axis, as the microshear bands. Light scattering from the curvature where the flow lines intersected the surface created the dark bands when the damage zone was viewed from the side. The spacing of the dark bands was determined by the angle of intersecting shear and the thickness of the specimen, and was the same for all the compositions that exhibited this shear mode. At a slightly higher stress (60.3 MPa), the PC/SAN 76/24 (194 layers) composite had necked. The cross section in Figure 15(b) shows that the flow lines of intersecting shear stabilized into a neck that propagated with thinning of both PC and SAN layers.

DISCUSSION

Combination of SAN, a glassy, relatively brittle polymer, with PC, a ductile glassy polymer, produced microlayer composites with mechanical properties intermediate between those of the two components. The transition from brittle failure dominated by cavitation mechanisms to ductile failure dominated by shear modes depended on the relative amounts of SAN and PC, but was also strongly affected by thickness of the alternating layers that comprised the composite. A macroscopic failure map was constructed to show the transition as a function of both composition and the number of layers in the composite (Fig. 16). Results of all the composites in the study were used to locate the lines that distinguish the brittle and ductile failure regimes, separated by a broad transitional region. The brittle-to-ductile transition achieved by increasing the amount of the ductile component is illustrated with 194-layer composites where there were examples of all
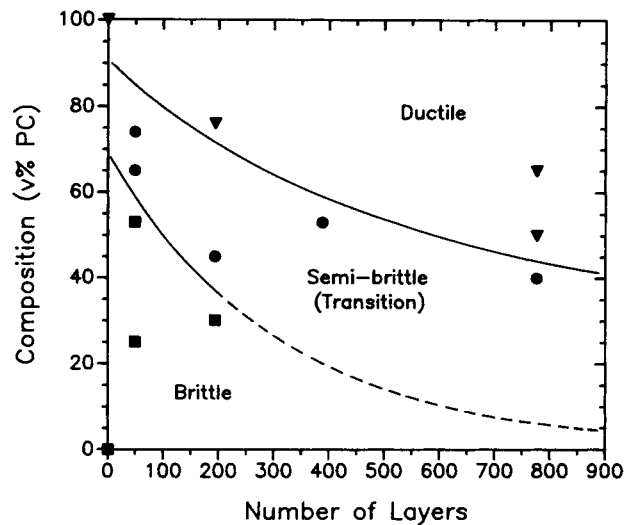
Figure 16 Failure regimes as a function of composite composition and the total number of layers in the composite.

three types of failure: brittle (PC/SAN 30/70), semi-brittle (PC/SAN 45/55), and ductile (PC/SAN 76/24).

The effect of layer thickness is shown in Figure 16 with three composites all having a composition of roughly equal amounts of PC and SAN but having different numbers of layers so that the thickness of individual SAN layers decreased from 22 μm to 5.4 μm to 1.2 μm. The failure mode was respectively brittle (PC/SAN 53/47, 49 layers), semi-brittle (PC/SAN 45/55, 194 layers), and ductile (PC/SAN 55/45, 776 layers). The boundary between the brittle and semi-brittle regimes could only be defined for composites with the lower number of layers since 388- and 776-layer compositions with the proportion of SAN high enough to impart brittle behavior were not available. However, from the trends that were observed, it could be predicted that the proportion of PC required for the transition from brittle to semi-brittle behavior would continue to decrease as the layers became thinner.

Interaction of cavitational and shear deformation mechanisms resulted in the transition from brittle to ductile failure. The role of size scale and interactions was apparent when the deformation processes were examined in the damage zone as it evolved at the notch root during tensile loading. The various damage mechanisms that were identified in the damage zone are summarized in Table IV for all the compositions. The sketches represent the appearance in the xy plane unless otherwise indicated. Internal notch crazing occurred in the SAN layers;

Table IV   Damage Mechanisms in Microlayer Composites of PC/SAN

Composition (PC/SAN v %, No. of Layers)	Internal Notch Crazes	Microshear Bands in PC (yz Plane)	Microshear Bands in SAN	Core Yielding	Internal Near-Notch Crazes	Intersecting Shear (yz Plane)	Neck Propagation (yz Plane)	Micro-delamination	Macro-delamination	Fracture Mode
0/100	✓									Brittle
25/75, 49	✓	✓						N.T[a]	N.T	Brittle
30/70, 194	✓	✓						N.T	N.T	Brittle
53/47, 49	✓	✓						N.T	N.T	Brittle
45/55, 194	✓	✓	✓	✓				C.Y[b]	C.Y	Transition
65/35, 49	✓	✓	✓	✓	✓			C.Y	C.Y	Transition
40/60, 776	✓	✓	✓	✓	✓	✓		C.Y	C.Y	Transition
74/26, 49	✓	✓	✓	✓	✓	✓		C.Y	C.Y	Transition
53/47, 338	✓	✓	✓	✓	✓	✓				Transition
55/45, 776	✓	✓	✓	✓	✓	✓	✓			Ductile
76/24, 194	✓	✓	✓	✓	✓	✓	✓			Ductile
67/33, 776	✓	✓	✓	✓		✓	✓			Ductile
100/0				✓			✓			Ductile

[a] At the notch tip.
[b] At the tip of the core-yielding zone.

stress concentrations created by the internal notch crazes led to two types of microshear banding: in the PC layers as a result of the stress concentration at the SAN-PC interface, and in the SAN layer at the craze tip (columns 1–3 in Table IV). Shear yielding was also observed at the notch root, and the stress concentration at the tip of the resulting plastic zone was responsible for the formation of near-notch crazes (columns 4 and 5). Global necking was observed in the initial stage as intersecting shear (column 6) and finally as the stable neck (column 7). At higher stresses, both microdelamination and macrodelamination mechanisms were observed (columns 8 and 9).

The initial irreversible deformation mechanism exhibited by a material under a particular stress state is a characteristic of the material. The response of both SAN and PC under the triaxial-tensile stress state achieved at a semicircular notch has been described.[4,5] A comparison of the conditions for internal-notch crazing of SAN and shear yielding of PC predicted that if the simple rule of mixtures applies, the initial irreversible deformation mechanism in the microlayer composites would be internal-notch crazing of the SAN layers.[1] This was observed: near the end of the linear region in the stress-displacement curve, crazes initiated at the notch surface in the SAN layers of all the compositions including the most ductile ones (Table IV). In the most brittle composites, the continued growth of internal-notch crazes, until fracture, was the dominant feature of the damage zone. Although some interaction of cavitational and shear processes was evident at the microscale when microshear bands initiated in the PC layers at the craze tips, failure was dominated by cavitation of the SAN component. Macrodelamination starting at the notch surface was also observed at stresses close to fracture.

Transitional behavior was represented by the semi-brittle compositions with major elements of both cavitational and shear deformation. The semi-brittle compositions were characterized by the appearance of a macroscopic shear-yielding mode superimposed on the notch crazes. When the shear-yielding condition of PC was achieved at the notch root, core yielding was observed as two families of intersecting slip lines that grew out from the notch surface. Interaction at the macroscale of the core-yielding mode with SAN crazing was inferred from the appearance of a second family of internal crazes ahead of the notch near the position of the tip of the plastic core-yielding zone. At higher stresses, the dilational stress concentration at the tip of the plastic zone also caused a macrodelamination crack in the center of the specimen.

At the microscale, shear deformation was observed in the SAN layers of the semi-brittle compositions (Table IV). Some of the internal-notch crazes ceased to grow when they terminated in microshear bands in the SAN layer. Although the conditions for this type of microshear banding in the SAN layers have not been determined, it may be the consequence of local stress redistribution at the tip of the craze produced by microshear bands in the PC layers. In the two most brittle of the semi-brittle compositions, only a few crazes terminated by this shear process, enough crazes grew away from the notch to define a craze zone that could be analyzed for the craze-growth condition, $\sigma_{m,c}$. Growth of the craze zone continued until these compositions fractured.

Craze termination by microshear bands in the SAN layer became increasingly prevalent as the composite ductility increased. In the other three semi-brittle compositions, all the notch crazes terminated in this way. The various lengths of the crazes when they terminated created such an irregularly-shaped zone that it was not possible to define a crescent shape from the craze tips for analysis of the craze-growth condition. When the notch crazes terminated in SAN microshear bands, growth of the damage zone occurred by initiation and growth of near-notch crazes. When the critical condition for growth of either notch crazes or near-notch crazes was determined, it was characteristic that the remote stress required for craze growth increased as the layer thickness decreased. Finally, a second macroscopic shear-yielding mode, intersecting shear, was observed. Global necking of PC follows from this through-thickness shear-yielding mode, but neck formation in the microlayer composites required large local deformation of the SAN layers along with the PC layers. The semi-brittle compositions fractured before the intersecting shear mode stabilized into a neck.

The ductile composites included those with the highest proportion of PC and the largest number of layers. Cavitational mechanisms were almost totally absent in these compositions; the internal-notch crazes that initiated at the notch surface terminated before growing any appreciable distance. The major feature that differentiated the ductile compositions was stabilization of intersecting shear into a neck that propagated with thinning of both PC and SAN layers. Stabilization of the neck in the ductile compositions was the result of a cooperative microshear process that became significant when the thickness of the SAN layers was on the micron-size scale.[2] This cooperative deformation process was apparent in cross sections of the damage zone as microshear

bands that initiated at internal crazes and grew through a number of alternating PC and SAN layers. The transition from cavitation to shear deformation of the SAN facilitated thinning of the SAN layers when the microshear bands subsequently coalesced into the macroscopic flow lines of intersecting shear.

CONCLUSIONS

The brittle-to-ductile transition in coextruded microlayer composites that consisted of alternating layers of PC and SAN was examined in the triaxial-tensile stress state achieved at a semicircular notch. Analysis of the damage zone that formed at the notch root during slow tensile loading led to the following conclusions:

1. The initial irreversible deformation process observed in all the composites was initiation of internal-notch crazes in the SAN layers. In the brittle composites, which included those with the highest proportion of SAN and the fewest number of layers, continued growth of internal-notch crazes until fracture was the dominant feature of the damage zone.
2. A second group of composites exhibited semi-brittle behavior that was transitional between brittle and ductile. At the macroscale both cavitational mechanisms and shear-yielding modes were observed in these compositions, while at the microscale interaction of crazing and shear banding had a major influence on the failure behavior.

3. The ductile composites included those with the highest proportion of PC and the largest number of layers. Cavitational mechanisms were almost totally absent due to cooperative shear banding of both PC and SAN. At the macroscale, deformation was dominated by the shear-yielding modes characteristic of PC that resulted in global necking.

REFERENCES

1. E. Shin, A. Hiltner, and E. Baer, *J. Appl. Polym. Sci.*, **47**, 245–267 (1993).
2. M. Ma, K. Vijayan, J. Im, A. Hiltner, and E. Baer, *J. Mater. Sci.*, **25**, 2039 (1990).
3. J. Im, A. Hiltner, and E. Baer, in *High Performance Polymers;* E. Baer and A. Moet, Eds., Hanser, New York, 1991, p. 175.
4. E. Shin, A. Hiltner, and E. Baer, *J. Appl. Polym. Sci.*, **46**, 213–230 (1992).
5. M. Ma, K. Vijayan, A. Hiltner, and E. Baer, *J. Mater. Sci.*, **24**, 2687 (1989).
6. B. L. Gregory, A. Siegmann, J. Im, A. Hiltner, and E. Baer, *J. Mater. Sci.*, **22**, 532 (1987).
7. A. Tse, E. Shin, A. Hiltner, and E. Baer, *J. Mater. Sci.*, **26**, 2823 (1991).
8. R. Hill, *The Mathematical Theory of Plasticity*, Clarendon, Oxford, 1950.